
21 STELLAR EVOLUTION: THE CORE

21.1 Useful References

- Prialnik, 2nd ed., Ch. 7

21.2 Introduction

It's finally time to combine much of what we've introduced in the past weeks to address the full narrative of stellar evolution. This sub-field of astrophysics traces the changes to stellar composition and structure on nuclear burning timescales (which can range from Gyr to seconds). We'll start with a fairly schematic overview – first of the core, where the action is, then zoom out to the view from the surface, where the physics in the core manifest themselves as observables via the equations of stellar structure (Sec. 15.5). Then in Sec. 22 we'll see how stellar evolution behaves in the rest of the star, and its observational consequences.

Critical in our discussion will be the density-temperature plane. For a given composition (which anyway doesn't vary too widely for many stars), a star's evolutionary state can be entirely determined solely by the conditions in the core, T_c and ρ_c . Fig. 39 introduces this plane, in which (as we will see) each particular stellar mass traces out a characteristic, parametric curve.⁸

21.3 The Core

There are several key ingredients for our "core view." These include:

⁸We will see that it costs us very little to populate Fig. 39; that is, there's no need to stress over the T - ρ price.

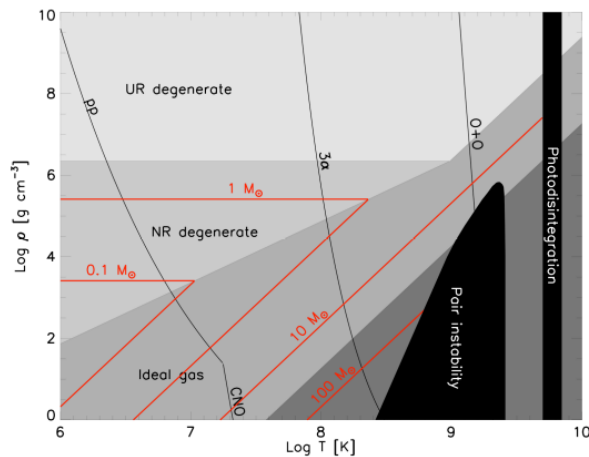


Figure 42: The plane of stellar density and temperature. See text for details.

- **Equation of State.** This could be an ideal gas ($P \propto \rho T$), a non-relativistic degenerate gas (Eq. 425, $P \propto \rho^{5/3}$), an ultra-relativistic degenerate gas (Eq. 428, $P \propto \rho^{4/3}$), or radiation pressure (Eq. 305; $P \propto T^4$). Which equation of state dominates depends on where we are in the (ρ_c, T_c) plane – see Fig. 39.
- **Nuclear Reactions.** The active nuclear reaction pathways, and related reaction rates, depend steeply on T and sometimes on ρ as well (as discussed in Sec. ??), with a general form of $\epsilon = \epsilon_0 \rho^\lambda T^\nu$. A given reaction pathway will “ignite” and rapidly start fusing when a given set of T and ρ are reached.
- **Energy Efficiency.** As we saw in Sec. 18.3 (see also Eq. 378), successively later stages of nuclear burning are incrementally less efficient. Each time the nuclear burning ratchets up to the next pathway, less and less binding energy can be liberated per nucleon. Thus τ_{nuc} of Eq. 254 gets shorter and shorter as the end draws near.
- **Stability.** In Sec. 16 we encountered several examples of stellar instabilities. For example, hydrostatic equilibrium breaks down for $\gamma_{ad} < 4/3$ (Eqs. 343 and 344). More generally, we will have to be on the lookout for cases when radiation pressure, degeneracy pressure, and/or ionization become particularly important; these will often correspond to significant dynamical upheavals in the star.
- **Nuclear Runaway.** Another kind of instability occurs if fusion occurs in a degenerate medium (we saw it at the end of Sec. 20). In this case we get a **fusion flash**: all available nuclear fuel is consumed on a thermal conduction timescale (just a few seconds) once burning begins.

21.4 Equations of State

Our discussion of stellar polytrope models (Sec. 17) is useful here for giving us a sense of what parts of Fig. 39 certain stars will occupy. What kind of polytrope? Because of the aforementioned stability constraints, for a star to be decently approximated by a polytrope requires

$$(464) \quad \frac{4}{3} < \gamma < \frac{5}{3}.$$

A useful relation comes from assuming a polytrope that is approximately in hydrostatic equilibrium. In this case, we obtain:

$$(465) \quad P_c = GM^{2/3} \rho^{4/3} (4\pi)^{1/3} F(n)$$

where $F(n)$ varies only slowly: from 0.233 to 0.145 for n in the range (1, 3.5).

Core is ideal gas

If we assume the core is an ideal gas, then this means

$$(466) \quad \frac{\rho_c k T_c}{\mu_e m_p} \approx \frac{1}{2} G M^{2/3} \rho_c^{4/3}.$$

Thus regardless of the evolutionary state, for a given star we have the relation

$$(467) \quad T_c \propto M^{2/3} \rho_c^{1/3}$$

or equivalently,

$$(468) \quad \log \rho_c = 3 \log T_c - 2 \log M + C.$$

Thus a star of given mass will lie along a diagonal line in the (logarithmic) plane of Fig. 39, with higher-mass stars lying increasingly toward the right (higher T). It seems that while lower-mass stars will approach and perhaps enter the degenerate regime, more massive stars never do.

Core is degenerate

For those stars whose cores do reach the (non-relativistic) degenerate zone, then degeneracy pressure must be responsible for Eq. 436's pressure calculated from stellar structure considerations. Thus

$$(469) \quad K_{NR} \rho_c^{5/3} \approx \frac{1}{2} G M^{2/3} \rho_c^{4/3}.$$

This result implies instead that

$$(470) \quad \rho_c \propto M^2.$$

or equivalently,

$$(471) \quad \log \rho_c = 2 \log M + C.$$

(Note that we would need to assume a somewhat different polytropic index to gain insight into the ultra-relativistic degenerate zone; but the non-relativistic assumption still gets the point across).

As we saw before, the structure of a degenerate object is independent of its temperature – so a degenerate core of a given mass has a fixed, maximum central density. Note that Eq. 441 also implies that a degenerate object's density increases as the square of its mass, which means that if we add mass to a degenerate white dwarf or neutron star its radius actually decreases. Furthermore, degenerate stars apparently lie along purely horizontal tracks in Fig. 39, with more massive stars at higher densities.

21.5 Nuclear Reactions

We've now seen how Fig. 39 can be populated with tracks representing the central conditions for a range of stars. We can now also populate the T - ρ diagram with a set of orthogonal curves describing nuclear energy production in the cores of our stars.

What is a useful characteristic energy production rate ϵ to use for these tracks? We know that in the absence of fusion, stars can be (briefly) heated via gravitational (Kelvin-Helmholtz) contraction. We'll therefore require that nuclear burning produces enough energy to overcome that contraction. In other words,

$$(472) \quad \tau_{KH} \sim \frac{GM^2/R}{L} \sim \frac{u}{\epsilon_V}$$

where

$$(473) \quad u = \frac{3}{2}nkT$$

and the volumetric and mass-based energy rates are related as

$$(474) \quad \epsilon_V = \epsilon_m \rho.$$

This implies that the relevant energy production rate of for any given fusion chain, and over a wide range of stars, is approximately

$$(475) \quad \epsilon_{m,0} \sim 10 \text{ erg g}^{-1} \text{ s}^{-1}.$$

We saw in Sec. ?? that the an approximate, general form of ϵ (Eq. ??) is

$$\epsilon = \epsilon_0 \rho^\lambda T^\nu.$$

Thus at the threshold $\epsilon_{m,0}$, we have

$$(476) \quad \log \rho = -\frac{\nu}{\lambda} \log T + \frac{1}{\lambda} \log \left(\frac{\epsilon_{m,0}}{\epsilon_0} \right).$$

Each reaction has its own corresponding coefficient. Successive stages of thermonuclear fusion turn on at higher temperatures and have steeper dependencies on T in particular (with $\lambda \gg 1$ only in the rarely-approached pyconuclear regime).

The features of these curves in Fig. 39 can then be described as follows:

- **p-p chain:** At high ρ , ignites at fairly low T . $\nu \approx 4$.
- **CNO cycle:** Dominates at sufficiently high T and low ρ . Thus given the right raw materials, CNO can actually ignite first as a cloud condenses to form a star. Still just converting protons into He, so continuous with the pp track, but now $\nu \approx 16$.
- **3 α :** Ignites at $\sim 10^8$ K, with a very steep T dependence: $\nu \approx 40$.

- **C+C**: Ignites at $\sim 6 \times 10^8$ K, with an even steeper (practically vertical) slope.
- **O+O**: Ignites at $\sim 10^9$ K, with an even steeper (practically vertical) slope.
- **Si**: Ignites at $\sim 2 \times 10^9$ K, with an even steeper (practically vertical) slope.

21.6 Stability

For any reasonable duration, dynamical stability will confine our stars to certain regions of the T - ρ diagram. In particular, our stars will become unstable whenever γ approaches $4/3$. Thus the “ideal gas” and “non-relativistic degenerate” zones are fair game, but in both the radiation-dominated regime and in the ultra-relativistic degenerate regime the conditions may verge perilously close to instability.

Other interesting instabilities can also develop. At the highest temperatures $T \gtrsim 10^9$ K, radiation pressure is often the dominant support. But the **pair instability** can remove or decrease that radiation support, leading to collapse. Instead of providing support,

$$(477) \quad \gamma \rightarrow e^+ + e^-$$

which means

$$(478) \quad kT \approx 2m_e c^2.$$

Since $1 \text{ eV} \sim 12,000 \text{ K}$ and $m_e = 0.5 \text{ MeV}$, this should set in at around

$$(479) \quad T_{pp} \approx 10^{10} \text{ K}.$$

In practice, pair instability sets in considerably earlier because the high-energy tail of the photon distribution can begin pair production long before the kT bulk of the photons reach that level, so it can be relevant for $T \gtrsim 5 \times 10^8$ K.

One final realm of instability is caused by **photodissociation of nuclei**. When $T \gtrsim 3 \times 10^9$ K, individual photons have enough energy to return all the lost binding energy back into heavy nuclei. The most important example is

$$(480) \quad \gamma + {}^{56}\text{Fe} \rightarrow 14 {}^4\text{He},$$

which plays an important role in supernovae of the most massive stars.

21.7 A schematic overview of stellar evolution

We’re finally in a position to piece together a basic-level astrophysical understanding of the evolution of a star. How do the central conditions of different objects evolve on the T - ρ diagram (Fig. 39).

- **One mass, one fate.** Each particular mass of star follows a distinct track, as described in Sec. 20.5.

- **Start low, end high.** We haven't talked much about the earliest stages of star formation, but we know space is big, empty, and cold. So any star presumably begins the earliest stages of its life at the relatively low temperatures and densities of the interstellar medium.
- **Move along home.** As a gas cloud approaches becoming a *bona fide* star, it contracts and radiates on the Kelvin-Helmholtz timescale (Sec. 14.5). As it contracts, no mass is lost so ρ must increase. And by the Virial Theorem (Eq. 266), T must increase as well.
- **Stop! in the name of fusion.** Eventually the core conditions will hit one of our fusion tracks. We defined our energy production tracks in Sec. 21.5 such that nuclear luminosity balanced the luminosity of gravitational collapse. So the star will remain \sim stable at this point for τ_{nuc} .
- **Get up again.** Once nuclear fuel is exhausted in the core, to maintain stability contraction must resume. ρ_c and T_c begin to increase again.
- **Rinse and repeat.** Pause at each nuclear burning threshold, for ever-briefer periods of time, until either a degenerate zone or unstable zone is reached.
- **Just fade away.** Once a star enters the non-relativistic degenerate zone, it's game over. Once any residual fusion is completed, the star can no longer contract to heat and support itself. It will just sit at constant ρ_c , gradually cooling and fading away: it is now a white dwarf. This is the fate of all stars with $M_* \lesssim 1.4M_\odot$, the **Chandrasekhar Mass**.
- **Do not burn.** Even lowest-mass "stars" will contract and evolve up and to the right in T - ρ space, but for $M \lesssim 0.08M_\odot$ the track will never intersect the pp-chain burning track. Thus they will become degenerate before ever undergoing fusion; these are **brown dwarfs**.
- **Your star is so massive...** The most massive stars will follow tracks along the upper border of the radiation-dominated regime. This border has the same slope as our equation-of-state tracks, implying that there is some maximum mass that stars can have – any more massive and they would reach $\gamma = 4/3$ and become entirely unstable.
- **Do not pass Go.** Fig. 39 also reveals the final, often-fatal fates of various stars. This includes:
 - Lowest-mass stars: these burn $H \rightarrow He$ for many Gyr, then become degenerate **Helium white dwarfs**.
 - Stars $< 1.4M_\odot \approx M_{Ch}$ produce He and then later also undergo the 3α process. They spend the rest of their days as **carbon/oxygen white dwarfs**.
 - These white dwarfs will occasionally evolve across an ignition line while inside the degenerate region. In this case, we have a **nuclear runaway** and the star will fuse all available fuel almost instantly

(on a thermal conduction timescale, just a few seconds). The best example is the **helium flash**, which occurs for stars at or just below $1M_{\odot}$. The 3α line is reached right near the non-relativistic degenerate zone, and the core luminosity will spike as high as $10^{11}L_{\odot}$ for a few seconds. This intense burst only slowly “leaks out” into observable regions, but it quickly melts away the core degeneracy.

- Stars $> M_{Ch}$ will succumb to the instabilities lurking at high T . Most will pass through multiple levels of fusion burning, all the way up to ^{56}Fe , before finally reaching the photodissociation threshold. They will die as **core-collapse supernovae**. The most massive stars are very rare, but some may end their lives via the pair-production instability instead.

21.8 *Timescales: Part Deux*

Note that our discussion so far has left out an explicit treatment of timescales: how long does a star sit at any given nuclear burning threshold, how long does it take to pass from one threshold to the next, and how long does it take a white dwarf to cool? For now, let’s merely realize that any given stage of fusion will continue for roughly τ_{nuc} (Eq. 254) while contraction occurs over roughly τ_{KH} (Eq. 252). So the Sun took only a few 10s of Myr to collapse from a gas cloud into a young zero-age main-sequence star, but it will sit on the H→He burning threshold for roughly 10^4 Myr. Since nuclear timescales scale roughly as M^{-3} , more massive stars will fuse up all available hydrogen in just a few 10s of Myr — the lowest-mass stars will take trillions ($> 10^6$ Myr!).

22 STELLAR EVOLUTION: THE REST OF THE PICTURE

We'll now consider stellar evolution from the external perspective. All the interior physics is now translated through millions of km of starstuff; Plato's cave doesn't have anything on this. As in Fig. 39 we will still observe stars move through a 2D space as their evolution goes on. But now, instead of T_c and ρ_c (which we can only infer and never directly measure) our new coordinates will be the external observables luminosity and effective temperature, L and T_{eff} . In truth even these quantities rely on inference at some level; so while the astrophysicist thinks of (L, T_{eff}) the observing astronomer will often think in terms of absolute magnitude (a proxy for L) and photometric colors (a proxy for T_{eff}). Yes, we've returned once again to the Hertzsprung-Russell diagram first introduced in Sec. 3.

22.1 Stages of Protostellar Evolution: The Narrative

The process of star formation is typically divided into a number of separate stages (which may or may not have distinct boundaries). Here, we will consider eight stages, beginning with the initial collapse (which we have already touched on) and ending when a star reaches what is known as the 'main se-

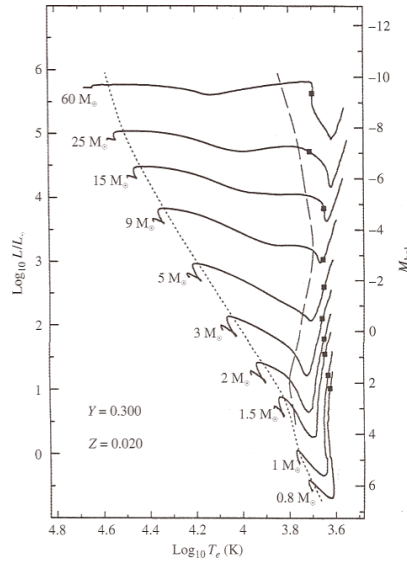


FIGURE 12.11 Classical pre-main-sequence evolutionary tracks computed for stars of various masses with the composition $X = 0.68$, $Y = 0.30$, and $Z = 0.02$. The direction of evolution on each track is generally from low effective temperature to high effective temperature (right to left). The mass of each model is indicated beside its evolutionary track. The square on each track indicates the onset of deuterium burning in these calculations. The long-dash line represents the point on each track where convection in the envelope stops and the envelope becomes purely radiative. The short-dash line marks the onset of convection in the core of the star. Contraction times for each track are given in Table 12.1. (Figure adapted from Bernasconi and Maeder, *Astron. Astrophys.*, 307, 829, 1996.)

Figure 43:

quence', or a stable state of central nuclear burning of Hydrogen, in which a star will remain for the majority of its life. Note that understanding all of the physics that go into these stages of evolution requires some knowledge of topics we have previously discussed: adiabatic processes (Sec. 15.4), convection (Sec. 16), and opacity (Section 11.1) to name a few.

1. **Gravitational Collapse** Initially, the collapse of our Jeans-mass fragment is isothermal: the temperature of the collapsing cloud does not change. The cloud starts at a low density and temperature, and so is optically thin in the infrared, allowing it to efficiently radiate away its collapse energy. However, as the density goes up, the dust grains get closer together until eventually the core becomes optically thick in the infrared, and collapse is halted by the increase in temperature (and thus gas pressure) as the energy from the gravitational collapse is trapped. (Note that theory says that this collapse is an inside-out process: the inner regions collapse faster than the outer regions, and so infall from the collapsing envelope continues during the next few stages). After this point, the core begins to contract nearly adiabatically (as it can no longer exchange heat efficiently with its environment) and continues to heat up as it slowly loses the energy it radiates away. The core will continue to heat up and contract roughly adiabatically, until it reaches a temperature of ~ 2000 K, and some of the energy briefly goes into dissociating all of the H_2 molecules into H, rather than heating the core, causing a second collapse. Once this is finished, the inner region again reaches hydrostatic equilibrium and resumes its slow, adiabatic contraction. This inner object is now referred to as a protostar.

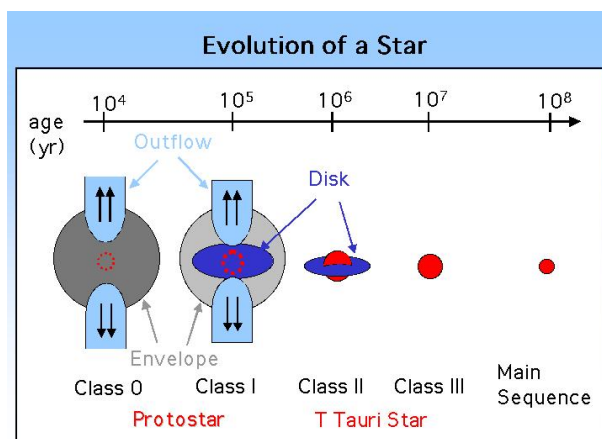


Figure 44: Schematic overview of the early stages of star formation and stellar evolution. (From <http://www-cr.scphys.kyoto-u.ac.jp/research/xray/press200011/figures/>, Apr 2019).

2. **Class 0 protostar** By this stage the envelope may still be collapsing, but a central core has formed which can be seen in cool dust emission at millimeter wavelengths. 'Class 0' is an observational classification indicating that warm dust emission from the core cannot yet be detected at infrared wavelengths. Essentially, the heat generated by the gravitational collapse and accretion has not yet significantly heated a large enough volume of the envelope to destroy the dust, lower the opacity, and make the warm inner regions visible in the infrared. However, there are other observable signatures that show a star is in the process of forming. One key structure that has begun to form at this stage is a flattened, rotating disk. This is a result of the conservation of angular momentum: the smaller the core gets, the faster it spins, causing the initially spherical core to flatten. This actually poses a problem for our forming protostar: if it cannot get rid of this angular momentum, it will never contract to the size of a star, because it would be spinning so fast that it would break up. The solution nature has come up with appears to be bipolar outflows, which begin to be seen at this stage. These rotating flows, launched from the disk (likely with help from the magnetic field, which has also gotten stronger due to conservation of magnetic flux as the cloud collapsed), are believed to carry excess angular momentum away from the system.
3. **Class 1 protostar** In contrast to a Class 0 source, infrared emission from the warm central disk can now be seen. However, material from the envelope is still sufficient to block the protostar from view at optical wavelengths. The outer envelope continues to collapse, infalling onto the central regions. The luminosity that is seen from the central source is largely powered by accretion of this material onto the disk and protostar (this energy comes from a shock, where gas that was in free-fall, traveling at large velocities, suddenly comes to a stop and deposits all of this kinetic energy). The disk continues to drive outflows to remove angular momentum, and by these later stages, now that the disk is larger and better organized, these outflows are better collimated and may even take the form of fast jets.
4. **Classical T-Tauri star (Class 2 protostar)**. The envelope is now sufficiently heated, depleted in mass from infall onto the disk, and/or blown away by the outflows that the central protostar can be seen at optical wavelengths. From this point on the disk will only get smaller as it accretes onto the star and is swept up into planets that are beginning to form. Accretion from the disk remains the primary source of luminosity for the protostar. This accretion is not a continuous process but is extremely stochastic, occurring in large bursts, and so the luminosity of the central object can vary substantially. The 'star' at this point is still much larger than its final radius, and continues to contract. It is also rotating quite quickly at this stage, with rotation periods often around a dozen days (despite its large size), compared to a month for the sun. Its central temperature continues to increase, and though it is still too low for hydrogen fusion, there may be deuterium fusion occurring

(though this does not generate a significant amount of luminosity compared to accretion). T-Tauri stars generally refer exclusively to low mass stars ($\lesssim \text{few } M_{\odot}$). Higher-mass analogues of these systems are known as Herbig Ae/Be stars.

5. **Weak-line T-Tauri star (Class 3 protostar).** By now, accretion onto the star is almost over (hence, only weak emission lines indicative of hot, accreting gas can be seen in the star's spectrum.) The disk is also only a residual remnant of its former self: exoplanets (especially large gas giant planets) should be well on their way to forming at this point. As the system changes from actively accreting to quiescently contracting, a 'transition disk' may be seen: these objects are expected to have large inner gaps due to planet formation that has cut off the supply of gas to the star, halting its further growth. Remnant disks, which may be mostly rock and dust, having very little gas, can be seen in excess infrared emission from the starlight captured by the dust and re-radiated as heat at longer wavelengths. Such debris disks can be understood as massive analogs of the Kuiper belt and zodiacal dust in our own solar system. These disks are observed to persist up to a few million years, telling us how long planets have to form before the raw materials for doing so are used up.
6. **Pre-main sequence star (Hayashi Track).** At some point during the T-Tauri phase, infall stops, and as we can clearly see the central object at optical wavelengths and place it on a Hertzsprung-Russell (HR) diagram (see Fig. 40), we now begin to refer to it as a 'pre-main sequence' star which has reached its final mass (though not yet its final radius). Once the star is no longer getting energy from accretion, its source of energy is just the potential energy released from its gravitational contraction. No matter the energy source, the large size of the star means that it is extremely bright at this point. Although the central star has for some time been too hot for dust to survive, it is still extremely optically thick. The primary source of its opacity is the H^- ion (see Sec. 11.1), which is an extremely temperature-dependent process: it is much more significant at lower temperatures than higher temperatures. The strong temperature dependency of this process causes the star to become convectively unstable throughout. This time, during which the pre-main sequence star is fully convective, in a state of convective equilibrium, and contracting toward its final size, is known as the **Hayashi track**. The star travels a nearly vertical path (nearly constant temperature) on the HR diagram (Fig. 40) until its central temperature becomes high enough for the core to become radiative rather than convective. As previously mentioned for the T-Tauri phase (which may overlap substantially with this phase) the star may already be fusing deuterium.
7. **Heney Track** (only for stars greater than $0.8 M_{\odot}$). Once a star's core becomes radiative, the star executes a sharp leftward turn on the HR diagram (Fig. 40). This occurs because the core is sufficiently hot for the

opacity to drop, which makes convection less efficient, and the core becomes fully radiative. The star reaches a new equilibrium, and depending on its mass, luminosity remains constant or increases slightly (for intermediate-mass stars), and the surface temperature increases slightly or substantially (for massive stars) as it continues to slowly contract. Stars less than $0.8 M_{\odot}$ never develop a radiative core, and so reach the main sequence immediately after the Hayashi track. Higher mass stars may spend very little time at all on the Hayashi track before they develop a radiative core and begin moving nearly horizontally across the HR diagram on the Henyey track. At the end of its time of the Henyey track, the star begins nuclear burning. However, as this process is not yet in equilibrium, the star continues to contract, moving down in luminosity toward its final location on the main sequence.

8. **Zero-age Main Sequence.** Once a star reaches the main sequence, it has now begun stable nuclear burning and reached an equilibrium between pressure from this source of energy generation, and gravity. The star will stay here for the majority of its lifetime (millions to billions of years) however, it will continue to slowly change: getting very slightly larger (and so brighter) as it ages. This leads to a famous problem known as the faint young sun paradox: when life on earth was developing, the sun was only $\sim 70\%$ as bright as its current luminosity, however we believe (since life developed) that there was still able to be liquid water on the earth's surface. Although this change in brightness might seem like a good way to determine the age of a star, it turns out that we need to precisely know the mass to do this, and we cannot directly the mass of a star unless it is in a binary system. Outside of stars in clusters (for which we can measure patterns in the positions of more massive stars on the HR diagram that are evolving into red giants), it is difficult to say more than that a star is on the main sequence (which could mean an age of anywhere from a few million to a few billion years!). Some clues can be seen in its spin rate and magnetic activity (both of which decrease), but we are currently limited, at best, to 10-15% accuracy (a fact which, for example, makes it difficult to construct understandings of the time evolution of exoplanetary systems).

22.2 Some Physical Rules of Thumb

Let's now dive into a deeper, more physical discussion of the processes involved. Here are a number of key bits we need to worry about:

- **Opacity vs. Temperature.** Fig. 42 gives a schematic view of what we expect here. Roughly speaking, we will have two extremes:

$$(481) \quad \kappa_R \propto \rho^{1/2} T^9 \text{ (below ionization)}$$

and

$$(482) \quad \kappa_R \propto \rho T^{-7/2} \text{ (above ionization; Kramer's Rule).}$$

- **Opacity vs. Thermal Gradient.** If κ is very low, radiation streams freely; otherwise, radiative transport of energy is very inefficient. So in the limit of very high opacity, energy will instead be transported by convection; based on the Schwarzschild stability criterion (Eq. 349) we expect

$$\frac{dT}{dr} = -\frac{T}{P} \left| \frac{dP}{dr} \right| \left(1 - \frac{1}{\gamma_{ad}} \right).$$

Otherwise, we are in the low-opacity limit and have a radiative profile. By the thermal profile equation (Eq. 282) we then expect

$$\frac{dT}{dr} = -\frac{3\rho\kappa L(r)}{64\pi\sigma_{SB}T^3r^2}.$$

- **Virial Theorem.** We saw that stars contract at various stages of their evolution. By Eq. 266, we should also expect that the rate of contraction is limited by a star's ability to radiate energy from its surface.

1. High opacity \rightarrow convective \rightarrow slow contraction
2. Low opacity \rightarrow radiative \rightarrow rapid contraction

22.3 The Jeans mass and length

A particularly important application of the Virial Theorem, relevant to the earliest stages of star formation, is to determine the conditions required for a system to be slightly out of equilibrium such that it would tend toward

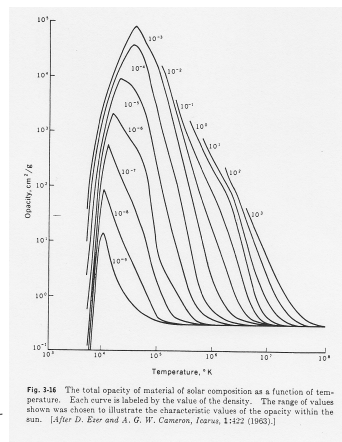
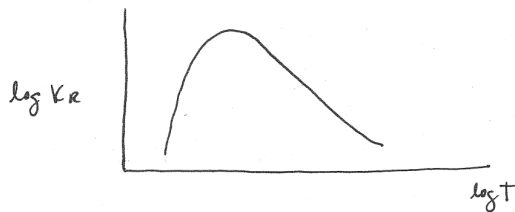


Fig. 3-16 The total opacity of material of solar composition as a function of temperature. Each curve is labeled by the value of the density. The range of values shown was chosen to illustrate the characteristic values of the opacity within the sun. [After D. Ezer and A. G. W. Cameron, *Journal*, 2:122 (1963).]

Figure 45: Opacity vs. temperature: *left*, schematic of the Rosseland mean opacity; *right*, an actual calculation (from Ezer and Cameron, 1963).

gravitational collapse or contraction. In this case, we would require that the magnitude of the potential energy term in Equation 256 be larger than the kinetic energy term.

Assuming that we are dealing with an ideal gas, and that we have a spherical, uniform density cloud we can write the total kinetic energy of all the particles in the cloud as

$$(483) \quad K = \frac{3}{2}NkT,$$

where N is the total number of particles in the system. The gravitational potential energy will be the same as Eq. 271,

$$U = -\frac{3}{5}\frac{GM^2}{R}$$

and so we can rewrite the Virial Theorem (Equation 256) as

$$(484) \quad \frac{3}{10}\frac{GM^2}{R} = \frac{3}{2}NkT.$$

the substitutions of $N = M/\bar{m}$ and $R = \left(\frac{3M}{4\pi\rho}\right)^{1/3}$, we can write

$$(485) \quad \frac{1}{5}GM^{2/3}\left(\frac{4\pi\rho}{3}\right)^{1/3} = \frac{kT}{\bar{m}}.$$

Solving Eq. 456 for M gives the mass at which a system will become gravitationally unstable: this is known as the Jeans Mass.

$$(486) \quad M_{\text{Jeans}} = \left(\frac{5kT}{G\bar{m}}\right)^{3/2} \left(\frac{3}{4\pi\rho}\right)^{1/2}$$

We can simplify this equation by scaling it to some typical conditions in the star-forming interstellar medium, and conveniently expressing it in Solar mass units.

$$(487) \quad M_{\text{Jeans}} = 2.3 M_{\odot} \left(\frac{T}{10 \text{ K}}\right)^{3/2} \left(\frac{n}{10^5 \text{ cm}^{-3}}\right)^{-1/2}$$

22.4 Time Scales Redux

The processes governing each of these stages of stellar evolution are subject to many of the same characteristic time scales that were introduced in Sec. 14.

Collapse and infall

Collapse and infall generally occur on a free-fall time scale (Eq. 245),

$$\tau_{ff} = \sqrt{\frac{3\pi}{32G\rho}}$$

which, as we discussed, is only ~ 30 min for the Sun. But before the Sun became a star its density was much lower. If we cast Eq. 245 in more familiar units, we have instead

$$(488) \quad \tau_{ff} = 2100\text{s} \left(\frac{R}{R_{\odot}} \right)^{3/2} \left(\frac{M}{M_{\odot}} \right)^{-1/2}$$

$$(489) \quad = 0.2\text{yr} \left(\frac{R}{1\text{AU}} \right)^{3/2} \left(\frac{M}{M_{\odot}} \right)^{-1/2}$$

$$(490) \quad = 0.6\text{Myr} \left(\frac{R}{0.1\text{pc}} \right)^{3/2} \left(\frac{M}{M_{\odot}} \right)^{-1/2}$$

So freefall times can be of order 0.1–1 Myr for solar-type stars.

Contraction

Contraction, in contrast, is governed by the time it takes for the star to radiate a significant amount of its gravitational potential energy. This is determined by the Kelvin-Helmholtz time scale (Eq. 252),

$$\tau_{KH} \sim \frac{GM_{\odot}^2}{R_{\odot}} \frac{1}{L_{\odot}}$$

which is roughly 3×10^7 yr for the Sun; longer for lower-mass bodies, and much shorter for more massive stars (see Sec. 14.5).

22.5 Protostellar Evolution: Some Physics

First, recall that it is much easier to measure luminosity L (from broadband photometry) and T_{eff} (from spectra) than it is to measure radii. But we can estimate R via Eq. 13,

$$(491) \quad L = 4\pi\sigma_{SB}R^2T_{\text{eff}}^2.$$

As we did with the tracks on the T - ρ diagram (Fig. 39), we will also lay out tracks on the H-R Diagram, Fig. 40. For example:

$$(492) \quad \log L = 2 \log R + 4 \log T_{\text{eff}} + C$$

Hayashi Track Revisited

The key ingredients are the following. First, once we reach the Hayashi track opacity is high, and the young objects are fully convective. Thus our equation of state is

$$(493) \quad P = \frac{\rho k T}{\mu m_p} = K_{\text{con}} \rho^{5/3}$$

Though contracting, we are still approximately in hydrostatic equilibrium – this is because contraction occurs on $\tau_{KH} > \tau_{ff}$. So we still have

$$(494) \quad \frac{dP}{dr} = -\frac{GM(r)}{r^2}\rho(r)$$

and optical depth is still given by

$$(495) \quad \frac{d\tau}{dr} = -\rho\kappa_R.$$

Combining the above two equations gives

$$(496) \quad \frac{dP}{d\tau} = \frac{GM(r)}{r^2} \frac{1}{\kappa_R}$$

and since temperatures are low at this point the star is mostly neutral and Eq. 452 gives the opacity:

$$\kappa_R \propto \rho^{1/2}T^9.$$

We then solve the above equations for $\tau = 2/3$ and $T = T_{\text{eff}}$ (see Sec. 13.3). The final solution is that along the Hayashi track (where stars are fully convective because opacity is high), we have

$$(497) \quad \log T_{\text{eff}} \approx 0.2 \log M + 0.05 \log L + C$$

or alternatively,

$$(498) \quad \log L \approx 20 \log T_{\text{eff}} - 4 \log M + C,$$

which matches up fairly well with the nearly-vertical Hayashi track seen on the right-hand side of Fig. 40.

Heney Track Revisited

As noted above, as the star contracts down the Hayashi track T_c and ρ_c will steadily increase. Eventually, the core will ionize and the opacity will drop (as shown in Fig. 42); as discussed previously in Sec. 16.4 the core will enter the radiative-support regime. At this point L may increase slightly but overall remains fairly constant – all the thermal energy eventually gets out.

With L roughly constant and R decreasing, this means

$$(499) \quad \log T_{\text{eff}} = 0.25 \log L - 0.5 \log R + C$$

must increase. So the star slides to the left along the Heney Track, leaving the Hayashi Track and heading toward the Main Sequence.

22.6 Stellar Evolution: End of the Line

So as we saw when discussing Fig. 39, stellar evolution as seen from the core is a tale of monotonic increases in central ρ and T . From the exterior, it is a story in two parts: each part governed by opacity, ionization, and the transition between convective and radiative interiors.

Once those central ρ and T increases sufficiently, nuclear fusion will begin either via the CNO cycle (for more massive stars) or the p-p chain (for stars of roughly Solar mass and below). In Sec. 19 we already detailed the various nuclear pathways that lead from those earliest stages of fusion to the final endpoints of stellar evolution.

When the central H fuel is finally exhausted, we've seen that the core will contract either until He fusion can be initiated, or until the core becomes degenerate (a He white dwarf). At this point, **shell burning** (Fig. 43) sets in and the star will actually go into reverse, re-ascending along first the Henyey and then the Hayashi track.

Recall that core burning is self-regulating and stable. As a non-degenerate core contracts slightly, its fusion energy production rate will increase dramatically – $\epsilon \propto T^4$ in the pp chain and $\propto T^{16}$ in the CNO cycle. This extra energy will heat the core, causing it to re-expand slightly, cool off, and so decrease the fusion rate.

In contrast, shell burning over a degenerate core is unstable. As fusion proceeds in the shell, the inert core mass grows. Since it is degenerate, by Eq. 441 as its mass increases its radius will decrease slightly. This contraction will compress and heat the fusing shell, leading to an accelerated fusion rate. Thus in shell burning, energy will be produced at a sufficiently rapid rate to essentially run Kelvin-Helmholtz contraction in reverse: the star's outer layers expand and cool off, entering a giant phase. This will initially be the **subgiant**

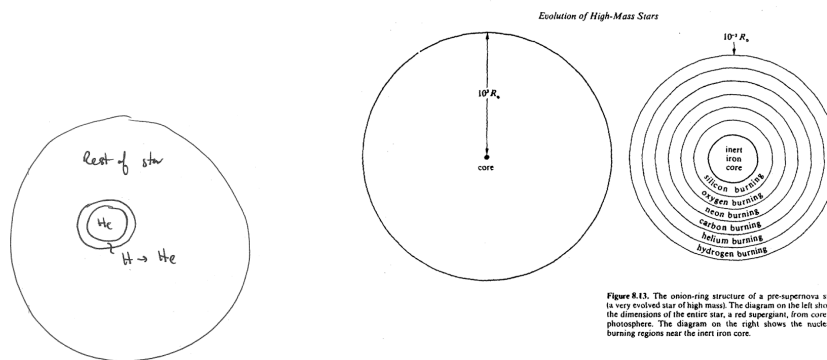


Figure 46. The onion-ring structure of a pre-supernova star is very evolved star of high mass. The diagram on the left shows the dimensions of the entire star, a red supergiant, from core to photosphere. The diagram on the right shows the nuclear-burning regions near the inert iron core.

Figure 46: Schematic pictures of shell burning: a degenerate He core surrounded by a thin burning shell surrounded by a mostly-H stellar envelope. Center and left panels are for an extremely massive star just before the end of its life; Note the linear scales of the two panels.

phase, essentially the reverse Henyey track, followed by the **red giant** phase, essentially a reverse Hayashi track.

22.7 *Red Giants and Cores*

Red Clump

When the core becomes sufficiently hot and dense (i.e. massive), the He in the core will begin to fuse. Most stars avoid the aforementioned helium flash, and undergo steady He fusion. Assuming that happens, the star's contraction along the red giant branch will pause so long as fuel remains for fusion to support the core against further contraction. Thus the star is once again in steady state, but due to He rather than H fusion. The star now sits on what is essentially a second main sequence, but powered by He burning. This phase lasts roughly 5% as long as the original main sequence lifetime. That seems short, but for the sun with a MS lifetime of 10 Gyr this means it will be a red giant for ~ 500 Myr – short, but $\sim 10\times$ longer than the Kelvin-Helmholtz timescale of expansion.

Because stars spend much more time in this region, they bunch up on the H-R diagram; this region is called the **red clump** and its (infrared) luminosity is roughly independent of composition, ages, etc. Because these giants are much brighter than the main sequence, their luminosities can more easily be measured and so this is often used as a “standard candle” to estimate the distance to a stellar population.

Asymptotic Giant Branch

After sitting on the red clump for a time, the (now carbon-rich) core will again become degenerate. It won't be quite hot and dense enough to initiate higher-order nuclear burning, but $\text{He}\rightarrow\text{C}$ fusion will continue in a shell around the degenerate C core. So it's the same story all over again: the core will grow in mass and (being degenerate) it will shrink, accelerating the burning process – the star is now undergoing a second phase of reverse-Kelvin-Helmholtz contraction (i.e., it is expanding) along the **asymptotic giant branch**. The star is not perturbed by quite as much as before, because there is still an intermediate layer of $\text{H}\rightarrow\text{He}$ fusion (via the CNO cycle) that is providing some energy.

As we briefly alluded to in Sec. 16.3, main-sequence stars hotter and more massive than the Sun have convective interiors beneath radiative envelopes. On the AGB, each fusing shell produces enough energy to exceed Eq. 349 and create its own local convection cell. This mixes the star's internal composition somewhat (it never becomes anywhere close to homogeneous); the star is said to be undergoing **dredge-up** of potentially interesting elements up to the observable surface layers.

Multiple fusion shells also tends to make a star unstable and leads to **stellar pulsations**, periodic expansions and contractions of the outer envelope of the star. These pulsations, combined with high luminosities and very low surface gravity, leads to considerable **mass loss** from the star in its later stages.

Escape velocity is given by

(500)

$$v_{\text{esc}} = \left(\frac{2GM}{R} \right)^{1/2}$$

(501)

$$v_{\text{esc}} = 620 \text{ km s}^{-1} \left(\frac{M}{M_{\odot}} \right)^{1/2} \left(\frac{R}{R_{\odot}} \right)^{-1/2}$$

(502)

which is then a factor of $\sim \sqrt{200}$ (or more) lower for the largest giants. Winds are indeed observed with Doppler shifts corresponding to about these velocities from evolved red giants and AGB stars.

Mass loss will eventually become sufficiently rapid that the entire envelope is lost to interstellar space; the exceedingly diffuse material around the star will eventually be observed as a **planetary nebula** (whose name is another historical anachronism). Only the degenerate core will remain; the star has finally become a **white dwarf**. This is the fate of all stars with initial masses $\lesssim 6M_{\odot}$.